Taylor & Francis
Taylor & Francis Group

AVIATION
ISSN 1648-7788 print / ISSN 1822-4180 online
2012 Volume 16(4): 115–123
doi: 10.3846/16487788.2012.753676

A NUMERICAL STUDY OF PARACHUTE INFLATION BASED ON A MIXED METHOD

Han Cheng[1], Li Yu[2], Wei Rong[3], He Jia[4]

[1, 2] College of Aerospace Engineering, Nanjing University of Aeronautics and Astronautics, Nanjing, China
[3, 4] Beijing Institute of Space Mechanics & Electricity, China Academy of Space Technology, Beijing, China
E-mails: [1]chenghanstorm@sina.com; [2]yuli_happy@163.com (corresponding author);
[3]rongweilxl@163.com; [4]chinajiah@163.com

Received 20 April 2012; accepted 22 October 2012

Han CHENG
Date of birth: 1984.
Education: College of Aerospace Engineering, Nanjing University of Aeronautics and Astronautics.
Research interests: fluid structure interaction, ADS design.
Publications: 6 research papers.
Present position: PhD student at Nanjing University of Aeronautics and Astronautics.

Li YU, *Prof PhD*
Date of birth: 1969.
Education: Nanjing University of Aeronautics and Astronautics. 2006–PhD (Eng.).
Affiliations and functions: member of Safety and Rescue Committee in CSAA; member of Return and Re-entry Committee in CSA; editor of "Spacecraft Recovery & Remote Sensing".
Research interests: fluid structure interaction, ADS design, environmental control systems.
Publications: over 30 research papers.
Present position: professor and doctoral tutor in College of Aerospace Engineering, Nanjing University of Aeronautics and Astronautics.

Wei RONG, *Prof PhD*
Date of birth: 1969.
Education: China Academy of Space Technology. 2008–PhD (Eng.).
Research interests: ADS design manned spacecraft, EDL system design.
Publications: over 40 research papers.
Present position: professor and doctoral tutor in Beijing Institute of Space Mechanics & Electricity, China Academy of Space Technology.

He JIA
Date of birth: 1983.
Education: M.Sc. (Eng.) degree from China Academy of Space Technology, 2006 to 2009.
Research interests: spacecraft ADS design, fluid structure interaction, EDL design and simulation.
Publications: over 10 articles and conference papers.
Present position: ADS design engineer at Beijing Institute of Space Mechanics & Electricity, China Academy of Space Technology.

Abstract. The C9 parachute was the research object in this work and was studied by using a fluid-structure interaction method and CFD method. An arbitrary Lagrangian-Eulerian method, a kind of fluid-structure interaction method, was used to simulate the inflation process. The dynamic relationship between canopy shape and flow field was obtained. The canopy shape in a stable phase was exported and was transformed into the porous media domain. Then the flow around the canopy shape was simulated by the CFD method we used based on the *k*-ε turbulence model. The experiments verified the accuracy of structural change and the feasibility of the porous media model. The arbitrary Lagrangian-Eulerian method not only can obtain the dynamic results of structure and flow field but also can provide a more accurate bluff body for further CFD analysis. The CFD method based on porous media and the turbulence model can obtain more detailed and accurate flow field results, which can be used as a complement to fluid-structure interaction analysis. This mixed method can improve the accuracy of analysis and be useful for other permeable fabric research.

Keywords: aerodynamic decelerator system, inflation process, fluid-structure interaction, porous media, parachute.

1. Introduction

A parachute is an important aerodynamic decelerator and is widely used in aviation, aerospace, weaponry, and other areas. The working style is simple, but the inflation is a typical interaction of structure and fluid that is a complex transient and nonlinear process (Yu, Ming 2007; Potvin *et al*. 2011). At present, parachute design is mainly based on empirical and semi-empirical formulas. The traditional design needs a large number of physical tests to verify. However, this approach not only consumes a lot of money but also extends the design cycle, which is not helpful for explaining the parachute inflation. Therefore, numerical simulation began to be applied for its economy and flexibility.

Fluid-structure interaction (FSI) methods, which are applied in aerodynamic decelerator system (ADS) research, have developed rapidly over the past few years. The representatives are arbitrary Lagrangian-Eulerian (ALE) method (Coquet *et al.* 2011; Tutt *et al.* 2011), the immersed boundary (IB) method (Kim, Peskin 2009), etc. (Kenji 2012; Potvin *et al*. 2011). Of these methods, the ALE method can fully consider fabric contact and material permeability and has been applied in actual design. However, this method consumes a large amount of computing resources, and the total number of elements must be controlled within some range. Moreover, since this method applied in most engineering practices is based on a laminar model (Coquet *et al*. 2011; Tutt *et al.* 2011), the results are rougher in calculating high Re number flow field.

CFD is another major simulation method, but how to get the canopy shape is a key problem. Canopy shape was generated from CAD software in most studies (Cao, Jiang 2007; McQuilling *et al.* 2011; Noetscher, Charles 2011) and was processed as a rigid body without permeability. Previous CFD methods have big differences from the actual engineering.

In this work, a C9 parachute, a typical flat parachute, is simulated by an FSI and CFD method. Firstly, the folded parachute inflating in an infinite mass case is simulated using LS-DYNA based on an ALE model. Then the inflated canopy shape is exported. Finally, the flow around this shape is simulated by using CFX based on porous media and the *k*-ε turbulence model.

2. FSI simulation

2.1. Finite element model

The C9 parachute is made of MIL-c-7020 type III fabric (Calvin 1984), and the parameters of the model are shown in table 1.

Table 1. Parameters of model

Structure of C9	Number of canopy gores	28
	Nominal diameter (m)	8.5
	Diameter of vent (m)	0.85
	Nominal area (m^2)	57.2
	Length of line (m)	7
Material properties of canopy	Density of canopy (kg/m^3)	533
	Young's modulus of canopy (pa)	4.3E + 8
	Thickness of canopy (m)	1E–4
	Linear resistance coefficient ($kg/m^3 \cdot s$)	1.6E + 6
	Quadratic resistance coefficient (kg/m^4)	4.8E + 5
Material properties of line	Density of line (kg/m^3)	462
	Young's modulus of line (pa)	9.7E + 10
Properties of air	Density of air (kg/m^3)	1.18
	Temperature of air (°)	25
	Ambient Pressure (pa)	1.01E + 5

This model is calculated in an infinite mass case based on the ALE method (the case in which deceleration effect can be negligible is called infinite mass case; otherwise it is called finite mass case; the latter not only considers the effect of flow field and structure but also considers the flight characteristics of the parachute; the latter needs a wider computational domain and is more sensitive to coupling coefficients than the former). A penalty function is applied to process the fabric contact. The principles and formulas describing the ALE method can be found in related papers (Souli *et al.* 2000; Casadei *et al.* 2001).

Figure 1 shows the finite element model based on ALE description. The lines and canopy are completely straightened, and the connection point of lines is fixed. The canopy looks like '*' from above. The canopy and lines are meshed by triangular elements (20,228) and bar elements (2,356). The hexahedral elements (147,392) are used to mesh the flow field. The canopy (Lagrangian description) and fluid domain (Eulerian description) interpenetrate with each other. The inlet boundary of the flow field is set as normal velocity inlet with a value of 80 m/s, and the others are shown in figure 2.

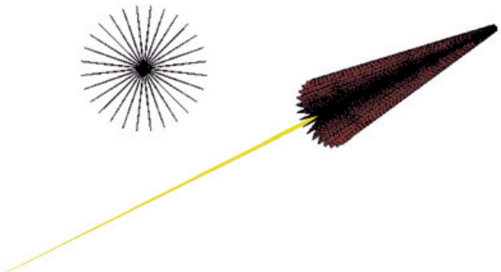

a) canopy and lines

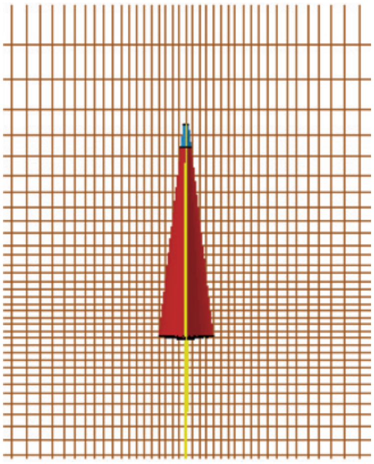

b) parachute and flow field

Fig. 1. Finite element model of parachute

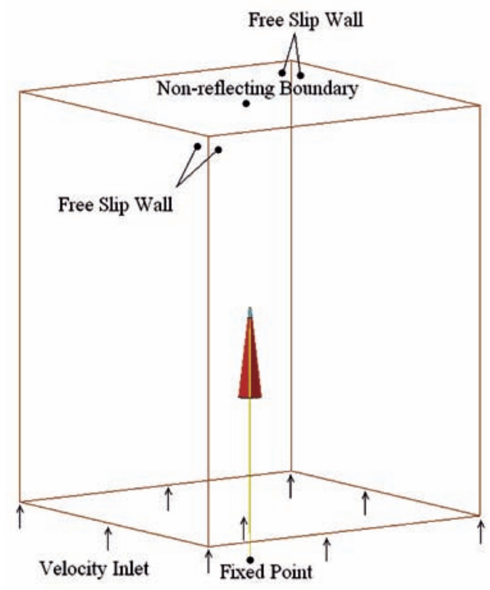

Fig. 2. Boundary conditions

2.2. Numerical results

The bottom of the canopy is inflated first, and a 'bottleneck' arises at the lower middle position of the canopy (Figs 3 and 4). As more air enters the canopy more quickly, the 'bottleneck' effect is aggravated and gradually moves to the top of the canopy (Fig. 5). Moreover, the velocity vector and the position of the high-pressure zone show that the air has difficulty flowing through the 'bottleneck' (Figs 3–5). Stress is therefore concentrated on the 'bottleneck' position.

The vent expands transiently when the 'bottleneck' moves to the top of the canopy (Fig. 6), and then the canopy has the classical 'squid' state (the 'squid' state is also called the 'bulb' state in some literature) (Wang 1997). The fully inflated area gradually expands to the bottom of the canopy, and inflation is completed at last (Figs 7 and 8). After the 'squid' state, the stress concentrates on the 'bulge' stably, and velocity and pressure remain stable.

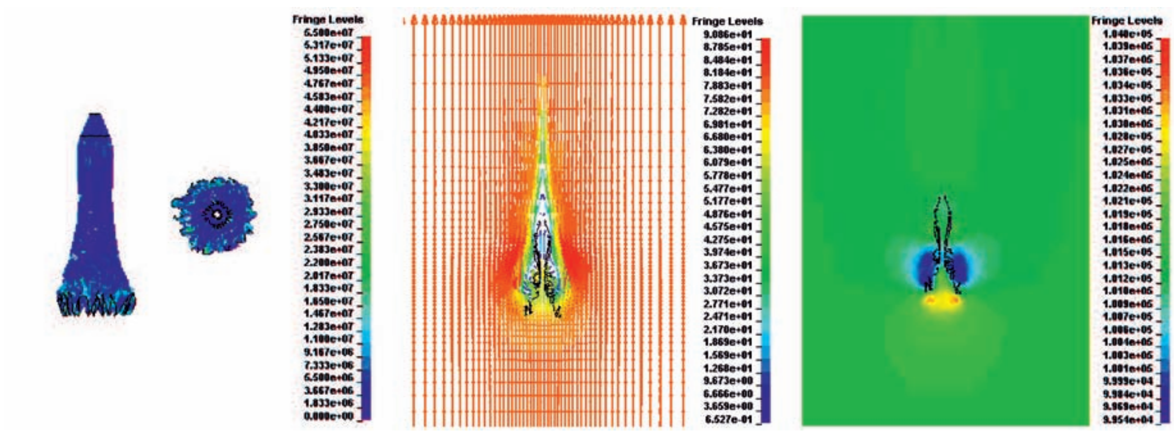

a) stress contour b) velocity vector c) pressure contour

Fig. 3. Structural and flow field results at t = 0.048 s

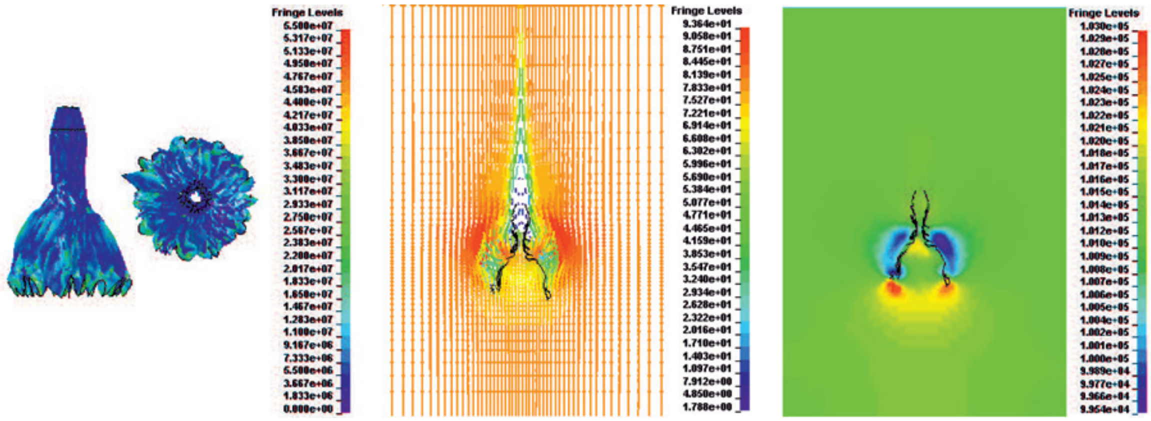

a) stress contour b) velocity vector c) pressure contour

Fig. 4. Structural and flow field results at t = 0.072 s

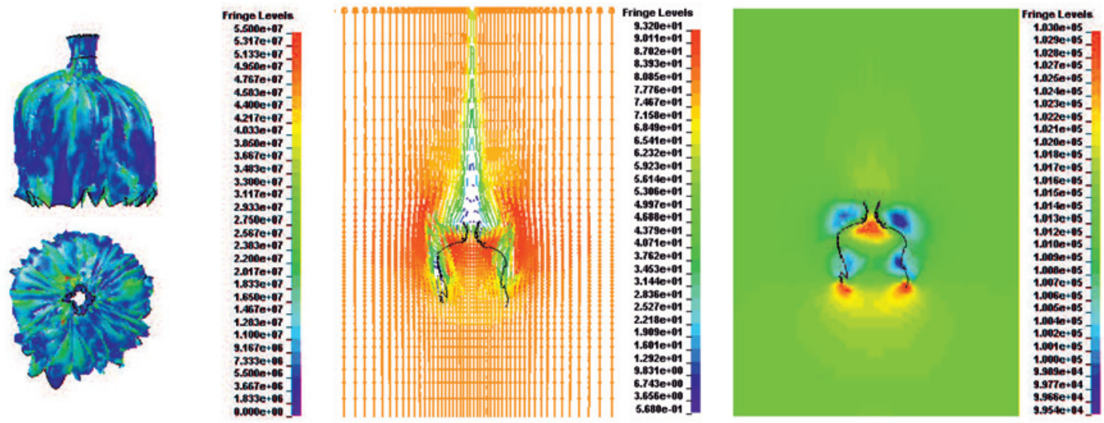

a) stress contour b) velocity vector c) pressure contour

Fig. 5. Structural and flow field results at t = 0.096 s

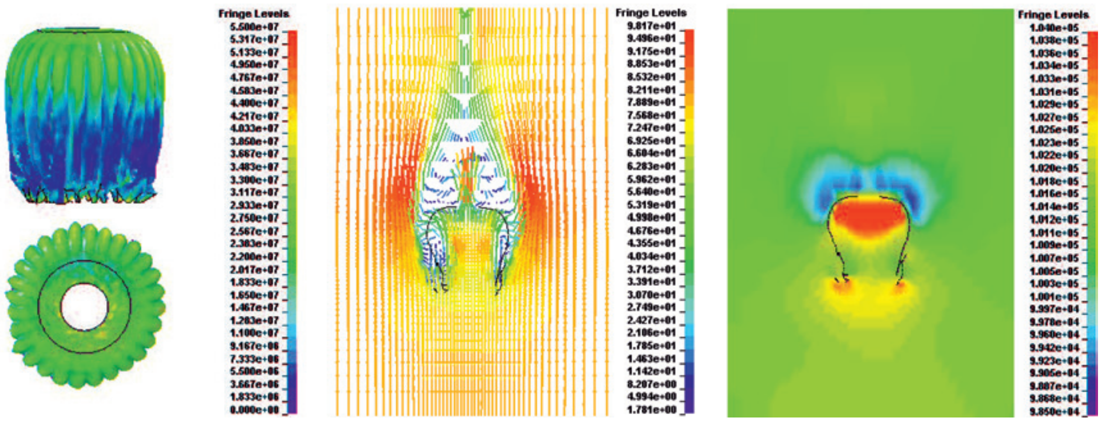

a) stress contour b) velocity vector c) pressure contour

Fig. 6. Structural and flow field results at t = 0.156 s

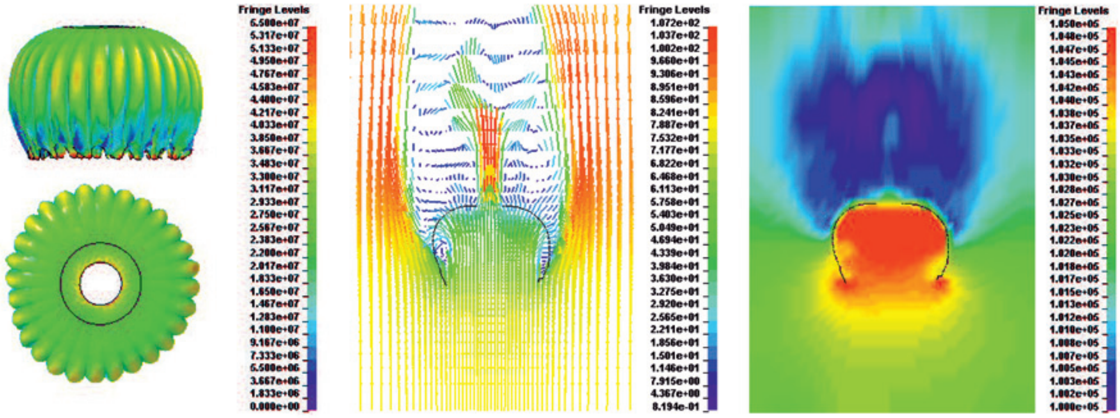

a) stress contour b) velocity vector c) pressure contour

Fig. 7. Structural and flow field results at t = 0.675 s

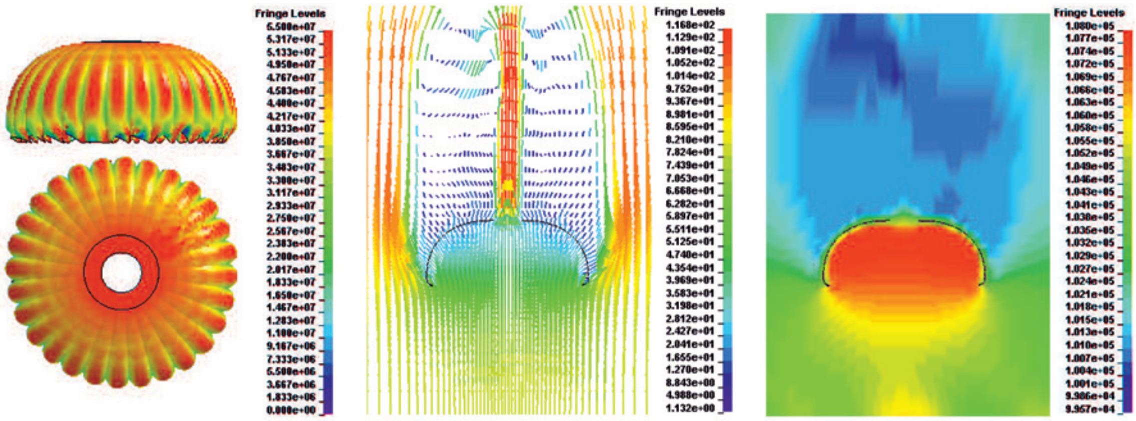

a) stress contour b) velocity vector c) pressure contour

Fig. 8. Structural and flow field results at t = 0.897 s

2.3. Comparison with experiment

The numerical results are compared with a related experiment (Fig. 9) in this paper. Both shape changes are similar; the 'bottleneck' moves from the bottom to the top and the non-inflating part is relaxed. The numerical results and experiment indicate that the essence of the 'bottleneck' is that the flow of air into the canopy is blocked. The 'bottleneck' effect only blocks the flow of air into the canopy, but does not restrain canopy movement.

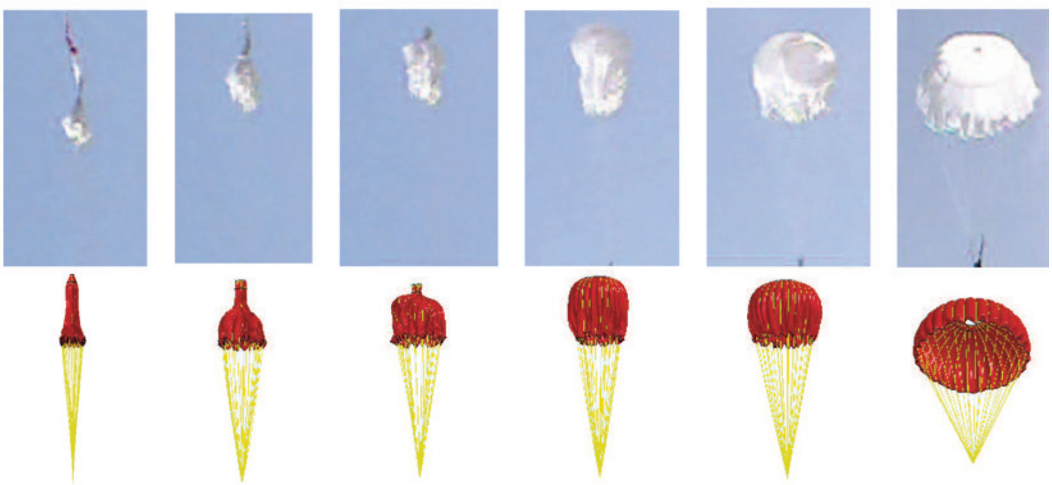

Fig. 9. Comparison between air drop test and calculation

3. CFD simulation

3.1. Verification of porous media model

In this section, the canopy is described by porous media domain. In order to reflect the permeability of MIL-c-7020 type III fabric (Aquelet *et al.* 2006), the linear resistance coefficient a ($a = \frac{\mu}{K_{pem}}$), quadratic resistance coefficient b ($b = K_{loss}\frac{\rho}{2}$), and thickness e are adjusted (Tab. 2). Đe new parameters are obtained based on the pressure drop equation:

$$\Delta P = \left(\frac{\mu}{K_{pem}}v' + K_{loss}\frac{\rho}{2}v'^2\right)\cdot e, \quad (1)$$

where μ is fluid viscosity, K_{pem} is the permeability coefficient of the medium, K_{loss} is the resistance-loss coefficient, ρ is the density of the fluid, v' is the permeability velocity, and e is the thickness of the medium.

Table 2. Permeability properties

	Đickness (m)	a (kg/m^3·s)	b (kg/m^4)
MIL-c-7020 III	1E-4	1.599E + 6	4.805E + 5
Porous media domain	3E-2	4.797E + 8	1.442E + 8

To verify the feasibility and accuracy of the CFD method based on the porous media model, a verification model is established according to a reference (Aquelet *et al.* 2006; Jia *et al.* 2009). Đe model and boundary conditions are shown in figure 10, and the differences are shown in table 3 (the model in Aquelet's work is called Model A for short, and the model established in this section is called Model B for short).

Table 4 shows the comparison of results in the same working conditions.

It can be seen that the relative errors of Model B are smaller than Model A and are controlled within 5%. Đe precision of Model B is stable and not affected by velocity change. Đerefore the porous media model can be used to simulate canopy permeability.

3.2. Model processing

At 0.879 s, the parachute has been inflated and is in a stable phase (Fig. 8). In this section, the canopy elements at that moment are exported from ALE results. Đe geometry is regenerated from the shell elements. Đen the geometry is cleaned up; some unnecessary fabric folds are removed (Fig. 11).

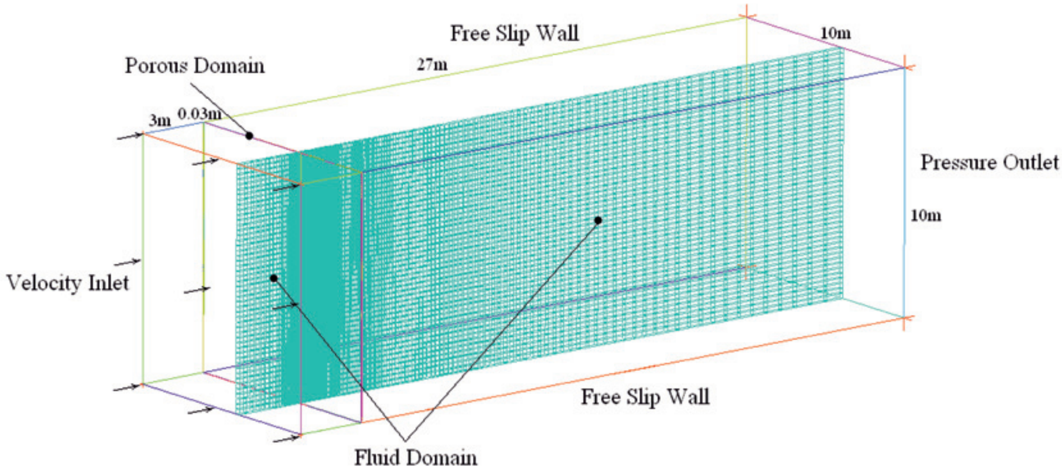

Fig. 10. Channel model

Table 3. Model differences

	Model A	Model B
Material of fabric (details in table 2)	MIL-c-7020 III	porous media domain
Element number of fabric	100	7500
Element number of fluid	3000	4.8E+5
Simulation method	ALE	CFD
Turbulence model	—	k-ε

Table 4. Comparison of results

Inflow velocity (m/s)	Permeability velocity (m/s)	Experimental pressure drop (Pa)	Model A		Model B	
			pressure drop (Pa)	relative errors (%)	pressure drop (Pa)	relative errors (%)
10	2.7	862	794	9	842	2.3
20	4	1628	1478	10	1523	4.9
30	5.4	2490	2316	7	2458	1.3
40	6.4	2969	3104	4	3037	2.3
50	7	3735	3653	2	3781	1.2

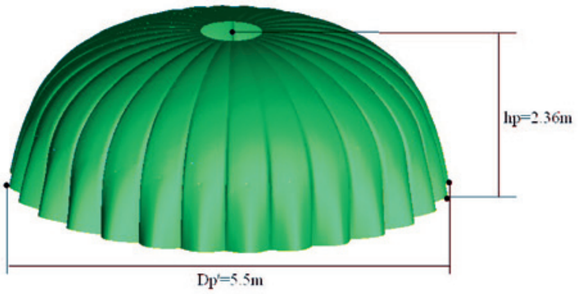

Fig. 11. Geometry after processing

Table 5. Comparison of geometry

	Experimental value (Ewing et al. 1988)	Exported value	Errors
D_p'/Nominal Diameter (D_0)	0.67	0.64	–4%
h_p/D_p'	0.41	0.43	4.9%
Project area of canopy (m^2)	25.5	26	2%

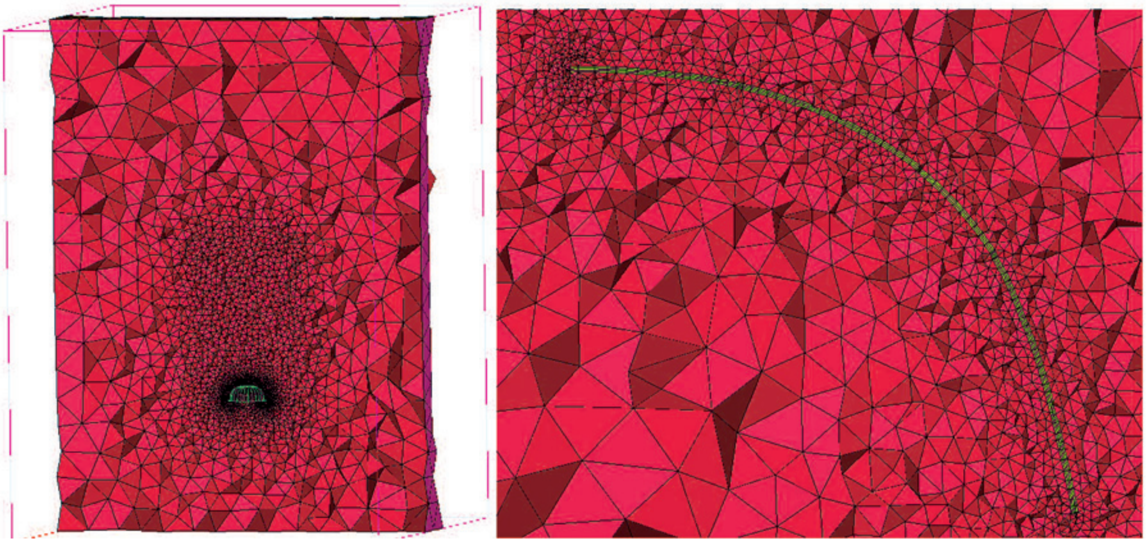

Fig. 12. Fluid domain and porous media domain (left: the whole; right: the enlarged)

The parameters in table 5, which describe the canopy shape, indicate that the geometry is the same as the actual shape. The details such as the bulge caused by airflow are clearly described, and the entire canopy looks like a bowl with a petal-like edge rather than a smooth hemisphere.

According to the geometry above (Fig. 11), the canopy is meshed by triangular elements (51,503). Then three layers of prismatic elements (154,509) are dragged based on those triangular elements. These prismatic elements are set as the porous media domain. The fluid domain, which surrounds the porous media domain, is meshed by tetrahedral elements (1,467,126). Figure 12 shows the model used in CFD simulation. The boundary conditions are the same as the test model (Fig. 10).

The incompressible steady-state simulation is solved by the fully coupled method. The turbulence model applied in the CFD simulation is the k-ε model. The principles and descriptions of the formulas of the k-ε model can be found in related works (Lin *et al.* 2005).

3.3. Results and analysis

Figure 13 shows the velocity vector and pressure contour of the CFD results.

From the results above, there exists a smaller velocity vector in porous media domain, which indicates weak airflow through the canopy surface. The weak airflow and the airflow around the canopy produce a small eddy near the canopy surface. The direction is opposite to the big eddy that is produced in the upper flow field of the parachute.

Compared with the results in figure 8, the results of the CFD method are more detailed and more accurate. Moreover, the drag coefficient, an important design parameter of ADS, is calculated based on this equation:

$$C_d = F_d / (\frac{1}{2} \cdot \rho \cdot v^2 \cdot S_o), \qquad (2)$$

where F_d is drag force, ρ is fluid density, v is velocity of airflow, and S_o is the area of the canopy.

Table 6 shows the drag characteristics. The drag coefficient calculated based on the CFD method is in agreement with the experimental data, while the value based on ALE is about 22.5% higher than the upper limit of the experimental value.

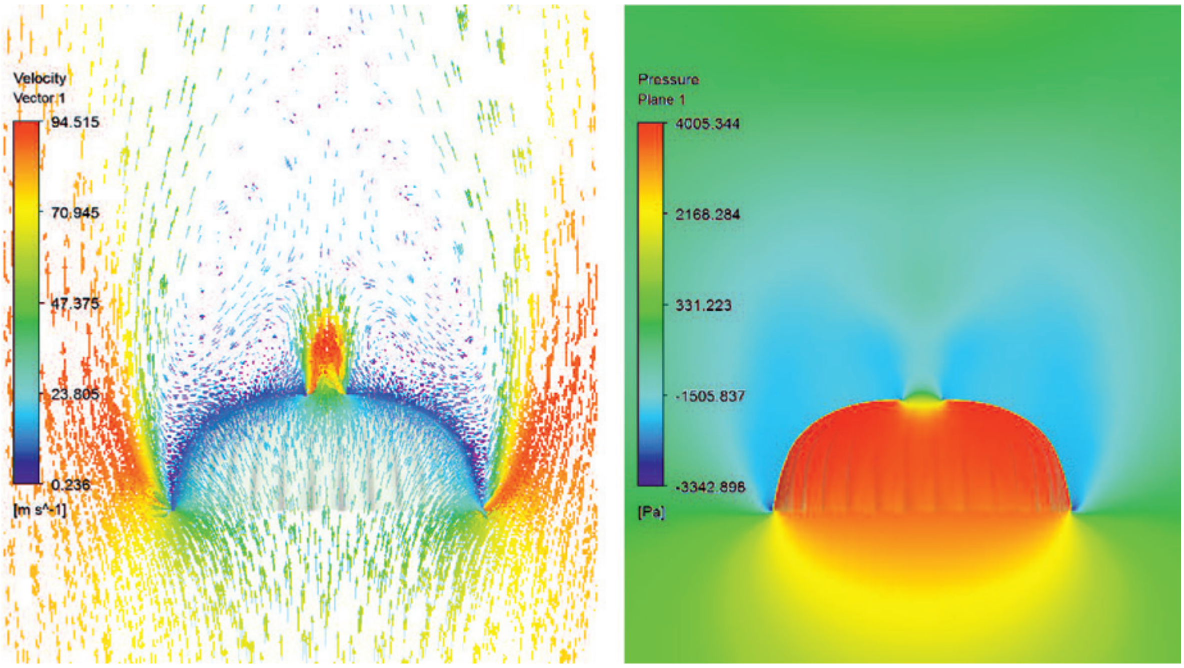

a) velocity vector b) pressure contour

Fig. 13. Flow field results based on CFD method

Table 6. Drag characteristics

Fluid density (kg/m^3)	Velocity (m/s)	Experimental value	Value based on ALE method	Value based on CFD method
1.18	80	0.75–0.8	0.98	0.8

These differences are mainly caused by these reasons:

a) the Lagrangian mesh (describing the canopy) and Eulerian mesh (describing the fluid domain) interpenetrate with each other in the ALE method, and the nodes on the interface need not be merged. This kind of pre-process is easy, but the mesh cannot be refined according to canopy shape. Since body-fitted mesh is applied in the CFD method, which can be refined according to the shape of the canopy, the CFD method can capture more flow field details;
b) the ALE method needs re-mapping almost every time step in transient calculation, and the amount of calculation is large. The total number of elements is limited by hardware conditions in engineering practice. However, this limitation is smaller in steady-state calculation based on the CFD method;
c) at present, the ALE method in most engineering applications and in this work is based on the laminar model. The accuracy would be affected in calculating high Re number flows.

4. Conclusions

In this work, the inflation process in an infinite mass case was simulated by the ALE method. Then the canopy shape in stable phase was exported for further flow-around analysis based on the CFD method. The conclusions are as follows:

a) the ALE method solves the fabric contact problem based on a penalty function and considers the fabric permeability. The inflation process of a folded parachute can be simulated more accurately. Moreover, the model pre-process is simple;
b) the ALE results can provide canopy shape for further analysis. The geometry exported from shell elements is more natural and realistic than the geometry generated from CAD software, which can improve the accuracy of numerical calculation;
c) porous media domain with a certain thickness can simulate the fabric permeability. Flow field results based on this model are different with those based on the traditional rigid model;
d) based on the same bluff body, the flow field results of the CFD method are more detailed and accurate than ALE results. Therefore the CFD method can be a complementary analysis for getting more accurate aerodynamic parameters.

However, the produce conditions of 'bottleneck' effect and how to use the CFD method to simulate the flow around the unexpanded canopy (Figs 3–7) need to be studied in the future.

Acknowledgments

This paper is supported by the National Natural Science Foundation of China (No. 11172137) and the Aeronautical Science Foundation of China (No. 20122910001). The authors are grateful to Piotr Strzelczyk and Zhuwei YIN for helpful suggestions. The authors are also grateful to Alan Hendrixson for his carefully polishing.

References

Aquelet, N.; Wang, J.; Tutt, B. A., *et al.* 2006. Euler-Lagrange coupling with deformable porous shells, in *ASME Pressure Vessels and Piping Division Conference,* 23–27, July, 2006, Vancouver, BC, Canada, ASME.

Calvin, K. L. 1984. Experimental investigation of full-scale and model parachute opening, *AIAA Report* 1984–0820.

Cao, Y. H.; Jiang, C. W. 2007. Numerical simulation of the flow field around parachute during terminal decent, *Aircraft Engineering and Aerospace Technology* 79(3): 268–272. http://dx.doi.org/10.1108/00022660710743877

Casadei, F.; Halleux, J. P.; Sala, A., *et al.* 2001. Transient fluid-structure interaction algorithms for large industrial applications, *Computer Methods in Applied Mechanics and Engineering* 190: 3081–3110. http://dx.doi.org/10.1016/S0045-7825(00)00383-2

Coquet, Y.; Bordenave, P.; Capmas, G., *et al.* 2011. Improvements in fluid structure interaction simulations of parachutes using LS-DYNA, *AIAA Report* 2011–2590.

Jia, H.; Rong, W.; Chen, G. L. 2009. The use of LS-DYNA to simulate the permeability parameters of the parachute canopy, *Spacecraft Recovery & Remote Sensing* 30(1): 15–20.

Kenji, T. 2012. Fluid structure interaction modelling of spacecraft parachutes for simulation-based design, *Journal of Applied Mechanics* 79: 1–9.

Kim, Y. S.; Peskin, C. S. 2009. 3-D parachute simulation by the immersed boundary method, *Computers and Fluids* 38: 1080–1090. http://dx.doi.org/10.1016/j.compfluid.2008.11.002

Lin, J. Z.; Ruan, X. D.; Chen, B. G., *et al.* 2005. *Fluid Mechanics*. Beijing: Tsinghua University Press. 324 p.

McQuilling, M.; Lobosky, L.; Sander, S. 2011. Computational investigation of flow around a parachute model, *Journal of Aircraft* 48(1): 34–41. http://dx.doi.org/10.2514/1.46255

Noetscher, G.; Charles, R. D. 2011. Benchmarking bluff body aerodynamics, *AIAA Report* 2011–2607.

Potvin, J.; Bergeron, K.; Brown, G., *et al.* 2011. The road ahead: a white paper on the development, testing and use of advanced numerical modelling for aerodynamic decelerator systems design and analysis, *AIAA Report* 2011–2501.

Souli, M.; Ouahsine, A.; Lewin, L. 2000. ALE formulation for fluid-structure interaction problems, *Computer Methods in Applied Mechanics and Engineering* 190: 659–675. http://dx.doi.org/10.1016/S0045-7825(99)00432-6

Tutt, B.; Roland, S.; Charles, R. D., *et al.* 2011. Finite mass simulation techniques in LS-DYNA, *AIAA Report* 2011–2501.

Wang, L. R. 1997. *Parachute Theory and Applications*. Beijing: Aerospace Press. 189–190 p.

Yu, L.; Ming, X. 2007. Study on transient aerodynamic characteristics of parachute opening process, *Acta Mechanica Sinica* 23(6): 627–633. http://dx.doi.org/10.1007/s10409-007-0112-3